A Sensor System to Monitor the Early-Stage Corrosion of A36 Carbon Steel

Dong CHEN[1,a,*], Max YEN[1,b], Paul LIN[1,c], Steve GROFF[1,d], Richard LAMPO[2,e], Michael MCINERNEY[2,f], Jeffrey RYAN[2,g]

[1]College of Engineering, Technology, and Computer Science, Indiana University-Purdue University, 2101 E Coliseum Blvd, Fort Wayne, IN 46805, USA

[2]U.S. Army Engineer Research & Development Center, Construction Engineering Research Laboratory, P.O. Box 9005, Champaign, IL 61826, USA

[a]chend@ipfw.edu, [b]yens@ipfw.edu, [c]lin@ipfw.edu, [d]groff.steve@gmail.com, [e]Richard.G.Lampo@usace.army.mil, [f]Michael.K.McInerney@usace.army.mil, [g]Jeffrey.P.Ryan@usace.army.mil

*Corresponding author

Keywords: Carbon Steel, Chloride, X-ray Diffraction, Rust, Corrosion Sensor.

Abstract. An innovative sensor containing A36 carbon steel was explored for corrosion monitoring. After being soaked in an aerated 0.2 M NaCl solution, the sensor's normalized electrical resistance (R/R_0) decreased continuously with the extent of corrosion from 1 to 0.64. Meanwhile, the sensor's normalized capacitance (C/C_0) increased continuously from 1.0 to 1.42. The sensors can be attached to a structure to be monitored via a wired or wireless network connection for automatic data acquisition, processing, storage and evaluation.

Introduction

Corrosion is an inherent problem which affects the construction, transportation, energy and many other industries. If corrosion is not monitored and correctly fixed, it could threaten public welfares and people's lives. Manual inspection of corrosion is costly, low efficient, subjective and sometimes dangerous. As a result, it is highly desirable to use corrosion sensors for automatic data collection, processing, and evaluation. Compared to manual inspections, automatic monitoring by corrosion sensors has significant advantages, such as promptness, comprehensiveness and efficiency. In addition, electrical signals from corrosion sensors are much easier to transmit, analyze and store than manual methods.

In this study, a corrosion sensor has been explored in order to find the systematic change in electrical properties of a metal (e.g., A36 carbon steel) during the early-stage of corrosion as it is exposed to a corrosive environment. During the course of corrosion and degradation, there is a change of the surface morphology and the electric conductivity of the metal, which is directly reflected by systematic changes of the capacitance and the resistance readings from the sensor. The sensor was powered by a 1.9 V and 1 kHz AC to minimize electrolysis and electrode polarization problems brought by a DC power. In practice, multiple sensors can be connected to a wired or wireless network for automatic data acquisition, processing and storage.

Experimental Methods

Cylindrical Capacitor

ASTM A36 steel was used in this study. As shown in Fig. 1, a cylindrical capacitor was created with the inner cylinder made from A36 carbon steel rod and the outer ring made from 316 stainless steel. Each of them had a height of 0.64 cm. The inner cylinder had a diameter of 1.27 cm while the outer ring had an outer diameter of 2.64 and inner diameter of 2.22 cm. The A36 carbon steel was polished by a 3M® 80 grit then a 3M® 600 grit sandpaper. Two wires were attached to the capacitor, one was soldered to the base of the center A36 steel rod and the other was welded to the

base of the outer ring of the 316 stainless steel. A bridge made of a glass substrate epoxy resin insulator from the circuit board (BM-FR4-1SS2, T-Tech Inc.) was adhered on the bottom of both the inner cylinder and the ring through a waterproof epoxy (15206 Anchor-Tite, Super Glue) to fix their relative positions. Finally, the waterproof epoxy was used to cover the connections of these wires as well as the base of the center rod to prevent corrosion of the connections and the wires. The uncovered A36 steel had 2.66 cm^2, which was subject to corrosion.

Similarly, a reference sensor was made following the same procedures and dimensions except replacing the A36 carbon steel rod with a 316 stainless steel rod of the same dimension, and then being welded to connect to the circuit-board bridge. The connections including welding points of the reference sensor were coated with waterproof epoxy (15206 Anchor-Tite, Super Glue) to prevent corrosion. The reference sensor was served to draw baseline information by addressing environmental conditions such as the temperature and the moisture level of air other than corrosion.

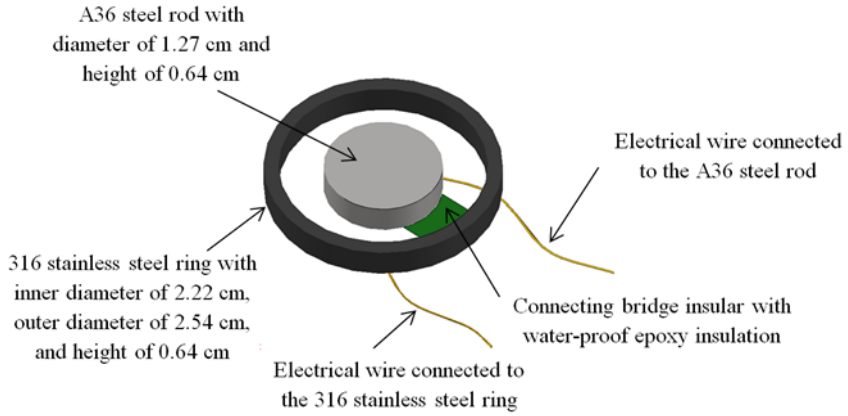

Fig. 1. Diagram of the corrosion sensor made of a cylindrical capacitor used for corrosion monitoring [1]

Corrosion Test

A 500-ml 0.2 M sodium chloride solution was used for corrosion testing. An air pump (Aqua Culture®) with a flow rate of ~1.2 L/min was continuously bubbling air through a diffuser to the solution to provide oxygen for the corrosion process. The air diffuser was porous sandstone. The dissolved oxygen level of the NaCl solution was maintained at around 8.8 mg/L. The corrosion sensor was submerged in the sodium chloride solution above the air diffuser. Every day during the course of the test, the sensor was removed from the solution, rinsed with DI water, dried at room temperature for 2~3 hours, and then tested with an automatic RCL meter (PM6303A, Fluke). At each measurement, multiple readings from the RCL meter with time were recorded until stable readings obtained, indicating the senor was dried with equilibrium to air moisture. As a result, the sensor experienced periodically wet/dry cycles twice a day for total 11 days. A new 0.2 M sodium chloride solution was made daily. The accumulated corrosion time of the senor in the sodium chloride solution was 225.5 hours. As a control test, a 316 stainless steel ring and the reference sensor was soaked in an aerated 500-mL 0.2 M sodium chloride solution separately to investigate the degree of corrosion of the 316 stainless steel and the reference sensor, respectively. The electrical resistance and the capacitance of the reference sensor were measured by the RCL meter following the same procedures as the corrosion sensor.

Sensor Measurements

The RCL meter was used to measure the resistance and the capacitance of the corrosion sensor in series mode, which was an available function of the meter. The meter used a frequency of 1 kHz and a voltage of 1.9 V for the measurements. In addition, the mass of the dried sensor was examined by a digital balance (ESA-3000, Salter-Brecknell) with a precision of 0.05 g. The initial weight of the corrosion sensor was 25.20 g. For the corrosion sensor, the initial resistance (R_0) in series was 7.24×10^6 Ω; the initial capacitance (C_0) in series was 9.2 pF before corrosion test. For the

stainless steel reference sensor, the initial resistance in series was 1.05×10^6 Ω, and the initial capacitance (C_0) in series was 25.6 pF.

Sample Analyses

After the corrosion sensor was removed from the NaCl solution, the daily solution samples were acidified with ACS grade nitric acid from Mallinckrodt to 10% (v/v) to dissolve the iron rust in the solution. Atomic Absorption Spectroscopy (AAnalyst 200, Perkin Elmer) was utilized to measure the dissolved iron in the solution.

Results and Discussion

Iron Loss During Corrosion

A new cylindrical corrosion sensor consisted of a rust-free A36 carbon steel rod in the center and a 316 stainless steel ring. During the corrosion test, the amount of iron in the solution was quantified by Atomic Absorption Spectroscopy after dissolution of the rust with nitric acid. At the end of the test of 225.5 hours, 3.24 mg of the accumulated iron was detected in the solution. The corresponding corrosion rate varied between 0.60 and 3.02 g/(m^2·d). It should be noted that there was rust on the A36 steel surface as well in addition to the amount found in the NaCl solution. The rust was not cleaned from the sensor intentionally to maintain its natural condition during corrosion process. However, for the control test of the 316 stainless steel ring alone or the stainless steel reference sensor, the dissolved iron concentration was less than 0.02 mg at the end of 225.5 hrs of corrosion, indicating the corrosion was insignificant.

Despite apparent corrosion of the A36 steel rod through visual inspections, the mass of the sensor was maintained constant at 25.20 ±0.05 g (i.e., variation was within ±0.2%) throughout the test. This result is consistent with the iron loss in the 0.2 M NaCl solution, which was within mg range. The minor change of the mass suggests the early-stage corrosion. The air gap distance between the A36 steel rod and the 316 stainless steel ring of the sensor did not increase, which is an important evidence for the explanation of the electrical resistance and the capacitance change of the sensor during corrosion in later discussions.

Compositions of the Rust

The corrosion of carbon steel occurs as an electrochemical reaction, with one anodic reaction and one cathodic reaction [2]. The anodic reaction represents loss of electrons from iron and the cathodic reaction describes the lost electrons accepted by oxygen. Our study by x-ray diffraction [1] show that three types of crystalline substances were found on the corroded steel surface, which were iron, lepidocrocite, and magnetite. Consistently, it is reported that the rust formed on steel surface is a mixture of lepidocrocite (γ-FeOOH), magnetite (Fe_3O_4), hematite (α-Fe_2O_3), goethite (α-FeOOH), and amorphous iron oxide [3,4,5]. The resistivity and the dielectric constant of the common rust materials, along with iron and air are listed in Table 1.

Tab. 1 Electrical resistivity and the dielectric constant of materials related to rust at ambient temperature [1].

Materials	α-Fe_2O_3	γ-FeOOH	Fe_3O_4	α-FeOOH	amorphous Fe_2O_3	iron	air
Electrical resistivity ρ (Ω m)	(1.58-5.62) $\times10^4$ [6]	(0.20-0.80) $\times10^5$ [7]	1.58×10^{-4} -0.1 [8]	(1.30-2.33) $\times10^5$ [7]	2.12×10^3 [9]	1.0×10^{-7}	4×10^{13}
Dielectric constant ε	12	2.6 [10]	20	11 [11]	4.5	-	1

Note: Data from reference [12] unless otherwise noted.

Electrical Resistance of the Sensor

Fig. 2 shows electrical resistance of the sensor in series (i.e., the measurement mode of the RCL meter) with an extension of corrosion time in the NaCl solution. The electrical resistance of the sensor decreased with the corrosion time. The normalized resistance of the sensor dropped from 1.0 to 0.64 after 225.5 hrs, a 36% decrease from the beginning.

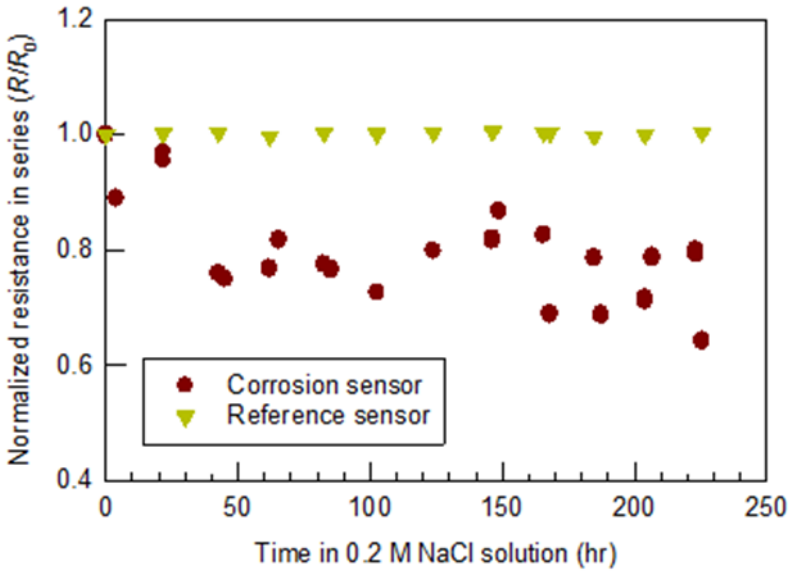

Fig. 2 Normalized electrical resistance in series (R/R_0) of the sensors vs. the accumulated time in the aerated 0.2 M NaCl solution

The electrical resistance is expressed by the following equation.

$$R = \frac{\rho l}{A}. \quad (1)$$

Where, R = electrical resistance of a material (Ω); ρ = electrical resistivity of the material (Ω m); l = the length of the material (m); A = the cross-sectional area of the material (m^2).

The resistance of the new corrosion sensor (before corrosion) is mainly due to the air gap between the center cylindrical A36 steel rod and the 316 stainless steel ring (see Fig. 1). Air has an electrical resistivity of 4×10^{13} Ω m [12]. When corrosion of the steel rod happened, rust formed a porous and loose structure [4] extended from the A36 steel surface to the surrounding air. As a result, the rust took a partial space that was previously occupied by air. In other words, after corrosion the gap between the A36 steel rod and the 316 stainless steel ring was partially filled with porous rust (small portion) and air (big portion). As mentioned earlier, the iron rust is a mixture of lepidocrocite (γ-FeOOH) and magnetite (Fe_3O_4), along with possible hematite (α-Fe_2O_3), goethite (α-FeOOH) and amorphous iron oxide [3,4,5]. Their electrical resistivity is shown in Table 1. As can be seen, the electrical resistivity of the rust components is at least eight orders of magnitude lower than air. According to Eq. 1, a lower electrical resistivity has smaller resistance. Consequently, the electrical resistance decreases with time or the extent of corrosion. Although spalling of rust from the sensor could enlarge the air gap between the A36 steel rod and the 316 stainless steel ring, the insignificant mass-loss result (i.e., mass change ≤0.2%) discussed earlier indicates this was not the case during the testing period of the early-stage corrosion. However, if significant spalling of rust happens and thus the air gap between the A36 steel rod and the 316 stainless steel ring increases, the trend of electrical resistivity might reverse (i.e. electrical resistance increases with time), suggesting much severe corrosion. In contrast, the electrical resistance of the stainless steel reference sensor was stable. In practice, the reference sensor can obtain the baseline signal of electrical resistances including the effects of air moisture and temperature, in order to identify the electrical resistance changes due to rust formation on the steel surface.

Capacitance of the Sensor

In addition to the electrical resistance, the capacitance of the sensor in series mode during corrosion was also examined. Again, capacitance in series was from the measurement mode of the RCL meter. Fig. 3 shows the change of the capacitance in series vs. accumulated time of corrosion in the aerated 0.2 M NaCl solution. A positive trend of the capacitance with the extent of corrosion was observed. More specifically, the normalized capacitance (C/C_0) in series increased from 1.0 at the beginning to 1.42 after 225.5 hours.

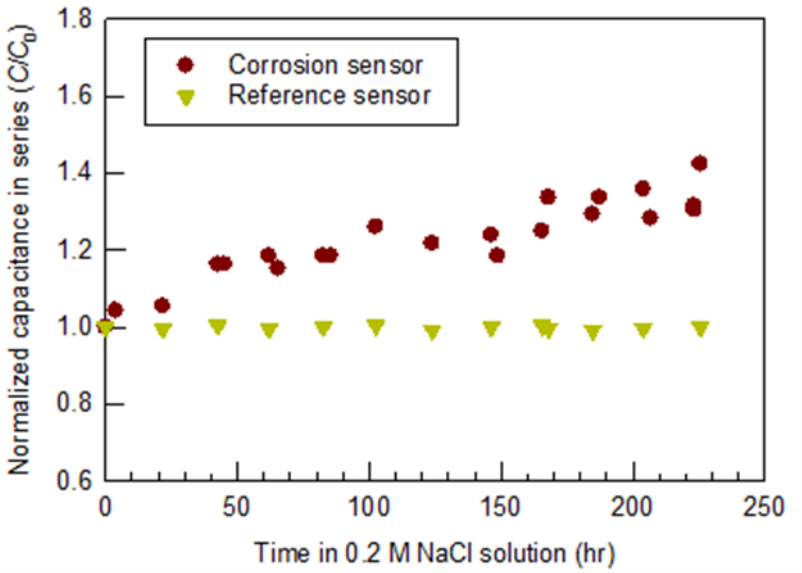

Fig. 3 Normalized capacitance in series (C/C_0) of the sensors vs. the accumulated time in the aerated 0.2 M NaCl solution

The capacitance of the sensor can be calculated from the following equation [13].

$$C = \frac{2\pi\varepsilon_0 h * \varepsilon}{\ln\left(\frac{b}{a}\right)} \quad (2)$$

Where, C = capacitance (F); ε_0 = free space permittivity, 8.85 pF/m; h = height of the cylinder sensor (m); ε = dielectric constant of the material(s) between the A36 steel rod and the 316 stainless steel ring; b = inner radius of the 316 stainless steel ring (m); a = radius of the A36 steel rod (m).

Before corrosion, air was between the A36 steel rod and the 316 stainless steel ring. Air has a dielectric constant ε of 1 [12]. After corrosion, rust was formed at the A36 steel surface. It means the space between the A36 steel rod and the 316 stainless steel ring was filled with both rust and air, although rust has a much smaller volume compared to air. As shown in Table 1, the dielectric constant ε of the substances composing the iron rust ranges from 2.6 to 20, much greater than air. Moreover, porous rust slightly increases the radius a of the A36 steel rod. As a result, an increase in both ε and a of the sensor raises the capacitance of the corrosion sensor, according to Eq. 2. Again, spalling of the rust from the A36 steel and thus a decrease of a was insignificant during the early-stage corrosion, because of the measured almost constant mass of the sensor during the test. Consequently, a higher capacitance reading in series reflects more rust formation at the A36 steel surface of the sensor during corrosion. Again, the reference sensor can be used to address the environmental factors (e.g., air moisture and temperature) caused capacitance changes other than corrosion.

Conclusions

This study explored a cylindrical corrosion sensor made of A36 carbon steel (representing the material of a structure or a system to be monitored for corrosion) and a 316 stainless steel ring

(representing an inert material of a low corrosion potential). A capacitor was formed with both metals separated by air. After corrosion in an aerated 0.2 M NaCl solution for 225.5 hours, the cylindrical corrosion sensor has shown a systematic decrease in the normalized electrical resistance (R/R_0) from 1.0 to 0.64. In the same time, the normalized capacitance (C/C_0) of the sensor increased from 1.0 to 1.42. However, the weight change of the sensor was within 0.2%, an indication of early-stage corrosion. Meanwhile, the reference senor, which was not subject to corrosion apparently, showed a stable normalized reading about 1.0. By attaching the corrosion sensors and the reference sensors with the identical passivation/coating to a steel structure, the extent of corrosion of the structure can be directly reflected by the electrical resistance decrease and/or capacitance increase of the sensor during the early-stage corrosion. Multiple corrosion sensors can be connected to a wired or wireless network for automatic data acquisition, processing, and evaluation.

Acknowledgements

The research project was funded by the US Army Engineer Research and Development Center, Construction Engineering Research Laboratory through the contract of W9132T-10-2-0056.

References

[1] D. Chen, M. Yen, P. Lin, S. Groff, R. Lampo, M. McInerney, J. Ryan, A corrosion sensor for monitoring the early-stage environmental corrosion of A36 carbon steel, Materials 7 (2014) 5746-5760.

[2] U.R. Evans, C.A.J. Taylor, Mechanism of atmospheric rusting, Corros. Sci. 12 (1972) 227-246.

[3] I. Suzuki, N. Masuko, Y. Hisamatsu, Electrochemical properties of iron rust, Corros. Sci. 19 (1979) 521-535.

[4] J.A. González, J.M. Miranda, E. Otero, S. Feliu, Effect of electrochemically reactive rust layers on the corrosion of steel in a $Ca(OH)_2$ solution, Corros. Sci. 49 (2007) 436-448.

[5] N. Nishimura, H. Katayama, K. Noda, T. Kodama, Electrochemical behavior of rust formed on carbon steel in a wet/dry environment containing chloride ions, Corrosion 56 (2000) 935-941.

[6] D. Varshney, A. Yogi, "Structural and electrical conductivity of Mn doped hematite (α-Fe_2O_3) phase, J. Mol. Struct. 995 (2011) 157-162.

[7] V. Lair, H. Antony, L. Legrand, A. Chaussé, Electrochemical reduction of ferric corrosion products and evaluation of galvanic coupling with iron, Corros. Sci. 48 (2006) 2050-2063.

[8] R. Ltai, M. Shibuya, T. Matsumura, G. Ishi, Electrical resistivity of magnetite anodes, J. Electrochem. Soc. 118 (1971) 1709-1711.

[9] A.A. Akl, Microstructure and electrical properties of iron oxide thin films deposited by spray pyrolysis, Appl. Surf. Sci. 221 (2004) 319-329.

[10] T.D. Glotch, G.R. Rossman, Mid-infrared reflectance spectra and optical constants of six iron oxide/oxyhydroxide phases, Icarus 204 (2009) 663-671.

[11] J.D. Filius, D.G. Lumsdon, J.C.L. Meeussen, T. Hiemstra1, W.H. Van Riemsdijk, Adsorption of fulvic acid on goethite, Geochim. Cosmochim. Ac. 64 (2000) 51-60.

[12] W.M. Haynes, CRC Handbook of Chemistry and Physics, 91st ed. CRC Press, Boca Raton, Florida, 2010.

[13] B.N. Basu, Electromagnetic Theory and Applications in Beam-Wave Electronics, World Scientific, Singapore, 1996, pp. 54.